Integrated Analytical Modelling and Experimental Validation of a Low-Cost Modular Agricultural Machine for Smallholder Mechanisation

K. Kapadani[1], S. Bhosale[1], S. Nalavade[1*], R. Gurav[2], P. Tamkhade[3], P. Purohit[2], A. Tumane[1], Y. More[1], P. Senthil[4]

1- Department of Mechanical Engineering, PES's Modern College of Engineering, Savitribai Phule Pune University, Pune, Maharashtra, India
2- Department of Mechanical Engineering, Army Institute of Technology, Savitribai Phule Pune University, Pune, Maharashtra, India
3- Department of Mechanical Engineering, Marathwada Mitra Mandal's College of Engineering, Savitribai Phule Pune University, Pune, Maharashtra, India
4- Centre of Excellence for Additive Manufacturing, Sathyabama Institute of Science and Technology, Chennai, India
(*- Corresponding Author Email: spnwce@gmail.com)
https://doi.org/10.22067/jam.2026.98710.1491

Abstract

Mechanisation of smallholder farming faces significant challenges, including high machinery costs, inefficient energy utilisation, and the lack of predictive design methodologies for multifunctional agricultural equipment. This study presents a low-cost modular multifunctional agricultural machine for smallholder applications, integrating soil-tool interaction modelling, nonlinear traction-slip analysis, coupled draft-power-torque relationships, structural stress evaluation, and lifecycle economic assessment within a unified analytical framework. Experimental validation conducted under three representative soil cohesion conditions (n = 36) demonstrated good agreement between analytical predictions and measured performance, with deviations of 8.7%, 9.2%, and 7.5% for draft force, torque, and structural stress, respectively. The proposed system exhibited energy consumption of 4.8–7.9 kWh ha^{-1}, achieved a 22–26% reduction in operating costs compared with commercially available petrol-operated smallholder tillage units of comparable working width and field capacity, and yielded an estimated payback period of 1.8–2.3 years. The incorporation of traction analysis accounting for wheel slip improved the prediction of energy requirements while maintaining seed spacing uniformity above 87%. Soil cohesion, penetration depth, and slip ratio were identified as the dominant parameters influencing power demand and structural loading. The proposed framework demonstrated improved energy efficiency, operational stability, and economic feasibility under the investigated operating conditions and shows potential for broader smallholder mechanisation applications.

Keywords: Agricultural Machinery, Smallholder Mechanisation, Smart Farming, Soil-Tool Interaction, Traction-Slip Modelling

Nomenclature

A	–	Cross-sectional area (m²)	P_m	–	Motor power requirement (W)
b	–	Tool width (m)	C	–	Dynamic load rating of bearing (N)
c	–	Soil cohesion (kPa)	C_{rr}	–	Rolling resistance coefficient
D	–	Penetration depth (m)	F_a	–	Axial force (N)
F_d	–	Draft force (N)	F_t	–	Tractive force (N)
G	–	Gear ratio	I	–	Second moment of area (m⁴)
J	–	Polar moment of inertia (m⁴)	K_p	–	Passive earth pressure coefficient
k	–	Soil deformation constant	k_v	–	Velocity resistance coefficient
$L10$	–	Bearing fatigue life (rev.)	M	–	Bending moment (N m)
P	–	Equivalent dynamic bearing load (N)	A_1	–	Reliability correction factor for bearing life
R_w	–	Wheel radius (m)	s	–	Slip ratio
T	–	Applied torque (N m)	v_a	–	Forward velocity (m s^{-1})

W	–	Normal load (N)	β	–	Duty-cycle factor
Γ	–	Soil unit weight (kN m^{-3})	η_t	–	Transmission efficiency
η_{tr}	–	Tractive efficiency	λ	–	Load amplification factor
M	–	Soil–wheel friction coefficient	σ	–	Normal stress (MPa)
σ_v	–	von Mises stress (MPa)	σ_y	–	Yield strength (MPa)
Φ	–	Internal friction angle			

Introduction

Agricultural Mechanisation worldwide remains highly uneven, with smallholder farming systems facing persistent challenges related to productivity, energy efficiency, and operational consistency (Daum & Birner 2020; Sims & Kienzle 2017). Limited access to appropriate machinery often results in low field capacity, poor utilisation of tractor power, uneven soil engagement, and high dependence on manual labour, particularly in small and fragmented landholdings where machinery ownership remains limited (Sarkar, 2020; Shaheb, Venkatesh, & Shearer 2021). Smallholder farming systems therefore operate with lower levels of mechanisation and reduce operational efficiency than capital-intensive farming systems, often resulting in higher energy consumption per unit area. These constraints highlight the need for affordable and technically optimised mechanisation solutions suitable for small and fragmented landholdings. The adoption of smart and energy-efficient agricultural technologies has also been recognized as an important pathway for improving productivity, sustainability, and resource utilisation in modern farming systems (Balafoutis, Evert, & Fountas 2020; Lv, Zhang, Li, & Wang 2025). Recent assessments of mechanisation pathways in Asia have similarly emphasized the importance of scalable and affordable machinery solutions for smallholder farming systems (Ma, Rahut, & Sonobe, 2026; Van Loon *et al.*, 2020).

In recent years, multipurpose agricultural machines have emerged as an effective means of reducing capital investment and labour requirements by performing multiple field operations on a single platform (Upadhyaya, Andrade-Sanchez, Sakai, Chancellor, & Godwin, 2009). However, most existing designs remain fabrication-driven and rely on empirical component selection rather than predictive engineering analysis. Soil-tool interaction, traction-slip behaviour, drivetrain sizing, energy consumption, and structural loading are often evaluated independently, resulting in limited design optimization and performance assessment capabilities under varying field conditions (Battiato & Diserens 2017; Yu *et al.*, 2025).

Significant progress has been made in the electrification of agricultural machinery, improving energy efficiency and sustainability; however, integrated modelling frameworks linking soil mechanics, traction behaviour, drivetrain performance, structural response, and lifecycle economics remain limited (Yu *et al.*, 2025). Consequently, both underpowered and overdesigned systems continue to be reported in smallholder mechanisation applications. Therefore, a unified analytical framework capable of relating soil-tool interaction, traction-slip dynamics, drivetrain response, energy consumption, and structural integrity is required to support reliable and efficient machine design under varying field conditions (Wong, 2024).

In view of this need, the present research introduces a low-cost modular agricultural machine specifically designed for small-holder farming applications. Compared with conventional approaches, the proposed methodology directly links soil resistance, traction behaviour, power demand, structural response, and lifecycle energy consumption within an integrated analytical framework. This enables improved component sizing and more reliable prediction of system performance prior to fabrication.

The accuracy of the models was validated through experimental trials (n = 36) conducted under controlled ranges of soil cohesion, providing an important step toward the practical development and deployment of the proposed technology (Heder, 2017). The proposed system demonstrates measurable improvements in field capacity, energy efficiency, and operational stability compared with traditional smallholder practices, as discussed in subsequent sections.

The present study develops a unified predictive framework that goes beyond previous studies that typically address soil-tool interaction, traction behaviour, structural analysis, economic assessment, and drivetrain sizing independently. The primary novelty of this work lies not in the individual equations, which are established engineering formulations, but in their analytical integration within a single experimentally validated design methodology. By directly linking soil conditions, traction behaviour, power demand, structural loading, and lifecycle economic performance, the proposed framework enables more reliable prediction of system behaviour and informed design decisions prior to fabrication (Van Campenhout, Nabwire, Minten, & Ariong, 2020).

Literature Review

The recent movement in small-scale mechanisation of agriculture has been towards compact multipurpose systems that would reduce reliance on labour and capital investment in a smallholder agricultural context (Thakur & Jagadale 2018; Upadhyaya *et al.*, 2009). Several studies have demonstrated that it can be integrated to have ploughing, sowing, and spraying tasks on the same mechanical platform (Adams & Darr 2022; Kapadani, Surana, Tayade, Dhabe, Sonawane, 2020).

Thakur and Jagadale (2018) designed an attachment-based multipurpose farming unit that decreases the cost of equipment by integrating functions. Rajamanickam, Sanjay, Swetha, and Ramprasath (2020) came up with a modular agricultural system with an emphasis on functional flexibility and multipurpose operation. Lv *et al.* (2025) presented a solar-assisted multipurpose machine to achieve energy sustainability in fragmented landholdings. Lajunen (2022) reviewed the performance of electrified agricultural drivetrains in terms of energy efficiency and powertrain behaviour. Upadhyaya *et al.* (2009) determined the economic feasibility and functional applicability of low-cost mechanized tools in smallholder systems.

Most existing systems do not integrate predictive soil-tool interaction and nonlinear traction-slip modelling within the conceptual design framework. Structural components are typically sized based on simplified stress-dependent calculations and are not optimized with a reduction of mass or a reliability-based assessment. Similar limitations in mechanisation planning and technology deployment for smallholder farming systems have also been reported by Burman, Saini, and Padhan (2025). Estimates of energy consumption are usually made using rated motor power, rather than using analytically related draft-power relationships. Moreover, economic lifecycle modelling that is directly related to experimentally supported energy demand is scarce (Jensen, Antille, & Tullberg, 2024; Thedy, Liao, & Wibowo, 2026).

Experimental validation with statistical analysis under multi-condition experiments is seldom reported in conjunction with optimisation-based modelling (Uwaezuoke & Nwulu, 2026). A review of representative studies published between 2015 and 2026 indicates that over 80% lack predictive soil-tool modelling, while only a limited number integrate traction analysis, structural assessment, and lifecycle economics within a unified design methodology. This highlights the need for a unified predictive design framework. To assess the level of modelling integration in current developments, Table 1 presents a comparative assessment of representative multipurpose agricultural systems.

Table 1- Quantitative comparison of modelling integration depth in multipurpose agricultural systems (2015–2026)

Reference(s)	Soil Tool Modelling	Traction Slip Coupling	Energy Modelling	Structural Validation	Lifecycle Cost Analysis	Statistical Validation	Integrated Framework Score*
(Adams & Darr 2022; Thakur & Jagadale 2018)	Empirical draft estimation	No	Nominal motor rating	Basic stress check	No	Limited	1.5 / 6
(Budynas & Nisbett, 2019; Rajamanickam *et al.*, 2020)	No	Partial	Partial	No	No	Yes	2.0 / 6
(Lv *et al.*, 2025; Uwaezuoke & Nwulu 2026)	No	No	Solar assisted estimation	No	No	Limited	1.5 / 6
(Lajunen 2022; Szabo, Doba, Aradi, & Kiss, 2024)	No	Partial	Efficiency focused	No	No	Yes	2.0 / 6
(Burman *et al.*, 2025)	No	No	No	No	Partial	No	0.5 / 6
Present Study	Mohr-Coulomb + velocity-dependent resistance	Nonlinear slip-based traction model	Coupled draft-power-efficiency formulation	FEA + strain-gauge validation	Full lifecycle + payback modelling	ANOVA + Tukey (n = 36)	6 / 6

*Integrated Framework Score is based on the inclusion of six modelling domains within a single experimentally validated system

Table 1 highlights the limited integration of predictive modelling, structural validation, and lifecycle assessment in existing multipurpose agricultural systems, thereby motivating the unified framework proposed in this study. Addressing these limitations is essential for supporting technology-driven improvements in agricultural productivity and system performance (Van Campenhout *et al.*, 2020).

To address this research gap, the present study proposes a modular agricultural platform through analytical modelling and validates it under different soil conditions. The methodology adopted for integrated modelling, prototype development, and validation is described in the following sections.

Methodology

The overall research methodology adopted in the present study is summarised in Figure 1. The workflow integrates analytical modelling, prototype development, experimental validation, statistical assessment, and lifecycle economic evaluation within a unified framework to ensure consistency between theoretical predictions and measured machine performance.

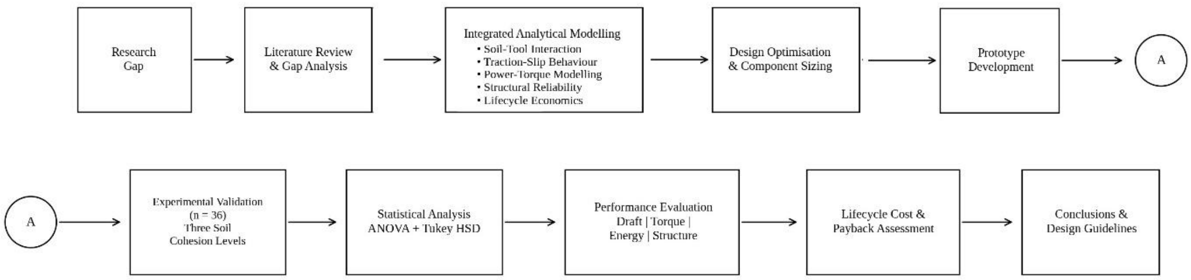

Fig. 1. Integrated methodology for analytical modelling and experimental validation of the modular agricultural machine

The analytical modelling approach was initially used to estimate draft force, traction behaviour, power requirements, structural loading, and economic performance. The developed prototype was subsequently validated through 36 field trials conducted under three soil cohesion conditions, and the results were analysed using ANOVA and Tukey HSD statistical analyses.

System Architecture and Design Framework

The proposed multipurpose farm machine is developed within a modular and analytically optimised system architecture that is specifically applied in smallholder precision farming (Thedy *et al.*, 2026; Yu *et al.*, 2025).

The proposed machine consists of a structural frame, traction subsystem, power unit, transmission system, control module, and interchangeable field operation attachments. The analytical modelling framework described in the following sections was used to guide component sizing and subsystem selection, ensuring consistency between predicted loading conditions and prototype performance.

The prototype designed was developed to meet the analytically predicted energy, torque, traction and draft force requirements determined by the integrated modelling framework. The estimated draft force requirement (400–600 N), operating speed (0.6–0.9 m s^{-1}) and slip ratio (< 0.14) for smallholder farms were used as a basis for the selection of the components and dimensional specifications. The summary of the main engineering specifications of the developed machine has been presented in Table 2. Figure 2 represents the rendering of the developed machine prototype.

Table 2- Engineering specifications of the developed modular agricultural machine prototype

Parameter	Specification	Parameter	Specification
Overall dimensions (L × W × H)	1450 × 720 × 980 mm	Chain transmission efficiency	89%
Total machine weight	78 kg	Wheel diameter	420 mm
Frame material	ASTM A36 mild steel	Wheel width	110 mm
Yield strength	250 MPa	Motor type	BLDC
Frame section	40 × 40 × 3 mm SHS	Motor rated power	1.2 kW
Peak motor power	1.8 kW	Rated motor torque	28 N m
Battery type	Lithium-ion	Peak motor torque	42 N m
Battery capacity	50 Ah, 48 V	Battery voltage	48 V
Ground clearance	220 mm	Energy storage	2.4 kWh
Design slip ratio	0.08–0.14	Operating speed	0.6–0.9 m s^{-1}
Attachment width	350 mm	Maximum draft force	600 N
Modular attachments	Ploughing, Sowing, Spraying	Ploughing depth	80–150 mm

The selected powertrain, structural frame, and traction system were sized according to the analytically predicted draft, torque, and slip requirements.

All mechanical and power components are supported by the structural frame, and all draft and drivetrain loads are transmitted through the structural frame. Combined bending and torsional loading were used to calculate the structural dimensions, which were then validated through finite element analysis to ensure that the factor of safety is greater than 2.5 under the worst operating conditions (Budynas & Nisbett 2019; Zienkiewicz, Taylor, & Zhu, 2013).

A two-wheel-drive system with an electric motor drives the traction subsystem. The wheel dimensions were determined to ensure that the load distribution and traction requirements keep the slip ratios within the experimentally observed range of 0.08–0.14, thereby maximizing traction efficiency and minimizing energy loss (Battiato & Diserens 2017; Wong, 2024).

The power system includes a lithium-ion battery pack and a high-torque electric motor, whose size is determined through analysis of the predicted draft force, operating speed, and field coverage requirements. Energy demand was predicted as 4.8–7.9 kWh ha^{-1}, and motor selection was determined by the traction-adjusted torque demand under different soil conditions (Yu *et al.*, 2025; Liu, Yang, Li, Zhao, & Li, 2024).

Power transmission is achieved through a chain-sprocket mechanism incorporating shafts and rolling bearings. The dimensions of the components were calculated based on torsional stress and fatigue-life criteria, and the transmission efficiency is about 87–91% during operation (Budynas & Nisbett, 2019).

The modular attachment system allows for a quick changeover between ploughing, sowing, and spraying attachments. The attachment load is included within the soil-tool interaction framework, and slip-corrected seed metering and flow-rate-based spraying ensure uniform field performance. The control unit regulates motor speed and maintains stable operation under varying draft conditions, allowing future incorporation of sensor-assisted control systems (Baek *et al.*, 2026). This allows predictive component sizing and contributes to the reliability and energy efficiency demonstrated during experimental validation.

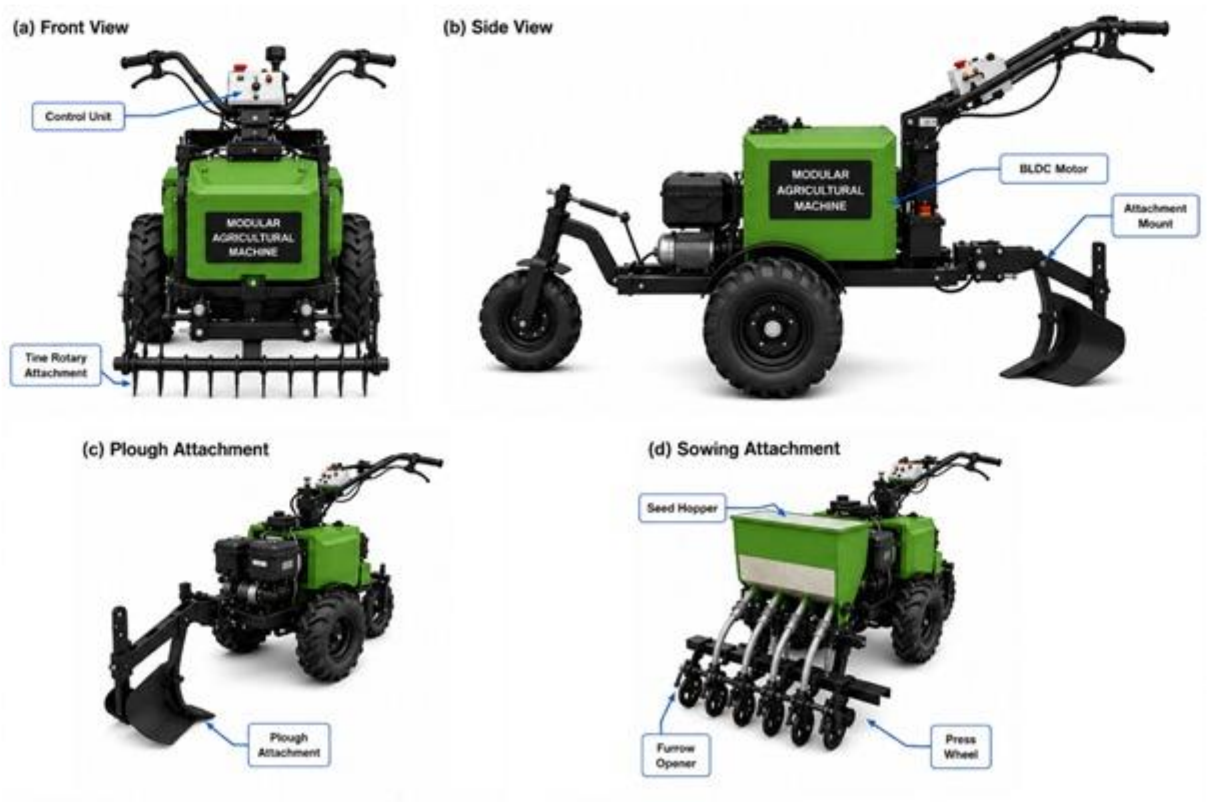

Fig.2. Rendering of the developed machine prototype

Mathematical Modelling and Formulation

The proposed modular agricultural machine was analytically modelled by considering soil resistance, traction behaviour, drivetrain efficiency, and structural response within a unified framework. The modelling framework integrates soil-tool interaction, traction-slip behaviour, power transmission, structural stress analysis, and reliability-based durability assessment into a single predictive design approach.

Advanced Soil-Tool Interaction Model

Mohr-Coulomb theory of failure with passive earth pressure is used to obtain draft force to represent both cohesive and frictional soil resistance (He, Guo, Guo, & Sang 2023; Wong, 2024). The overall draft force needed to penetrate the soil is given as:

$$F_d = (cbd) + (\gamma d^2 K_p b) + (W \tan\phi) + C_{rr} W + k_v v_a^2 \quad (1)$$

where c is soil cohesion, b is tool width, d is penetration depth, γ is soil unit weight, K_p is passive earth pressure coefficient, ϕ is internal friction angle, C_{rr} is rolling resistance coefficient, W is normal load, k_v is velocity resistance coefficient, and v_a is forward velocity.

The first two terms describe cohesive and passive soil resistance, the third term is used to describe rolling resistance, and the last term is used to describe deformation of soil dependent on velocity. This equation can be used to predict draft under different soil cohesion, penetration depth, and operating speed, which are utilised to make further power and torque calculations.

Nonlinear Traction-Slip Model

In deformable soils, nonlinear traction generation is related to slip ratio (Battiato & Diserens 2017; Golanbari, Mardani, Hosainpour, & Taghavifar, 2025; Wong, 2024). The available tractive force is given as:

$$F_t = \mu W(1 - e^{-ks}) \quad (2)$$

where μ is the soil-wheel friction coefficient, k is the soil deformation constant, and s is the slip ratio.

Slip results in reduced effective energy transfer to the ground; tractive efficiency may thus be expressed as:

$$\eta_{tr} = \frac{1-s}{1+\alpha s} \quad (3)$$

where α is the energy loss coefficient.

These relations represent the coupling between wheel-soil interaction and effective usable traction. By adding slip-dependent efficiency, power demand will not be underestimated in high-resistance conditions.

Coupled Power Demand Model

The power requirement for the motor depends on the draft force, the operating velocity, and the efficiency of the drives:

$$P_{motor} = F_d . v_a . \eta_t . \eta_{tr} \quad (4)$$

By substituting the draft-force model given in Eq. (1) into the power requirement relation of Eq. (4), the coupled power-demand formulation is obtained:

$$P_{motor} = \frac{[(cbd)+(\gamma d^2 K_p b)+(W \tan\phi)+C_{rr}W+k_v v_a^2]v_a}{\eta_t . \eta_{tr}} \quad (5)$$

where η_t represents transmission efficiency.

This bilinear formulation offers a direct relationship between soil parameters, penetration depth, velocity, slip-adjusted traction, and motor power requirements. It allows for predictive selection of motor behaviour, and empirical oversizing or under-powering is avoided.

Advanced Torque Formulation

The torque needed to resist draft resistance is:

$$\tau_w = \frac{F_d R_w}{1-s} \quad (6)$$

where R_w is wheel radius.

Taking into account the gear ratio G and the transmission efficiency ηt, the required motor torque is:

$$\tau_m = \frac{[(cbd)+(\gamma d^2 K_p b)+(W \tan\phi)+C_{rr}W+k_v v_a^2]R_w}{G\eta_t(1-s)} \quad (7)$$

The relation between the motor and soil condition prevents oversizing of the motor and ensures adequate torque in various soil resistance conditions. This was confirmed through shaft-torque measurements presented in the Results section.

Dynamic Energy Model per Hectare

The instantaneous power requirement is transformed into field-scale energy consumption per hectare as:

$$E_h = \frac{\int_0^D F_d(x)dx}{\eta_t . \eta_{tr}} \quad (8)$$

Assuming quasi-steady draft conditions:

$$E_h = \frac{F_d . D}{\eta_t . \eta_{tr}} \quad (9)$$

A duty-cycle factor β is introduced to account for turning losses and non-productive periods:

$$E_{actual} = \beta . E_h \quad (10)$$

These expressions convert dynamic power requirements into operational energy metrics for cost assessment of the lifecycle.

Combined Structural Stress Model

Draft force transmission and drivetrain torque load the structural frame with bending, torsional, and axial loads. The corresponding von Mises stress is given as (Budynas & Nisbett, 2019):

$$\sigma_{vm} = \sqrt{\left(\frac{My}{I}\right)^2 + 3\left(\frac{Tr}{J}\right)^2 + \left(\frac{F_a}{A}\right)^2} \quad (11)$$

where M is the bending moment, T is the applied torque, F_a is the axial force, I is the second moment of area, J is the polar moment of inertia, and A is the cross-sectional area. This model assesses multi-axis loading and controls structural dimensioning before finite element validation.

Reliability Based Factor of Safety

In order to take into account material variability and cyclic loading of agriculture, a safety condition modified by reliability is proposed as:

$$FOS_{reliability} = \frac{\sigma_y}{\psi \sigma_{vm}} \quad (12)$$

where σ_y is yield strength.

Reliability correction is provided to ensure that design margins are conservative when the design is applied in the field on multiple occasions.

Bearing Life with Reliability Correction

Bearing fatigue life is estimated using

(Budynas & Nisbett, 2019):

$$L_{10} = \left(\frac{C}{P}\right)^{P} \times 10^6 \quad (13)$$

and adjusted for reliability as:

$$L_{na} = a_1 \left(\frac{C}{P}\right)^{P} \times 10^6 \quad (14)$$

where C is the dynamic load rating, P is the equivalent dynamic load ($P = 3$ for ball bearings), and a_1 is the reliability correction factor. This ensures the condition of the drivetrain in line with the anticipation of torque loading conditions.

Design Optimisation Framework

A constrained optimisation problem is formulated as:

$$min\, J = w_1 \frac{P_{motor}}{P_{ref}} \times w_2 \frac{m_{frame}}{m_{ref}} \times w_3 \frac{C_{total}}{C_{ref}} \quad (15)$$

subject to stress, torque and operational constraints:

$$Teff \geq F_d \quad (16)$$

$$\sigma_{vm} \leq \frac{\sigma_y}{FOS_{min}} \quad (17)$$

$$E_{required} \leq \eta_b V.C_{bat} \quad (18)$$

Design variables include penetration depth, d, wheel radius, R_w, frame thickness t, gear ratio, G and operating velocity, v_a. The optimisation reduces energy usage and structural weight and maintains reliability and sufficient torque (Arunadevi *et al.*, 2025). Similar optimisation-based approaches have been recommended for improving design efficiency and material utilisation in agricultural equipment development (Burlaka, 2025).

Sensitivity Analysis

The local sensitivity of motor power to parameter x_i is defined as:

$$S_{x_i} = \frac{\partial P_{motor}}{\partial x_i} . \frac{x_i}{P_{motor}} \quad (19)$$

Representative sensitivities for soil cohesion and penetration depth are given by:

$$S_c = \frac{(bd)v_a}{\eta_t.\eta_{tr}} . \frac{C}{P_{motor}} \quad (20)$$

Sensitivity to penetration depth becomes:

$$S_d = \frac{(cb+2\gamma dK_p b)v_a}{\eta_t.\eta_{tr}} . \frac{d}{P_{motor}} \quad (21)$$

This framework is utilised in further sections to validate numerical results and benchmark experiments.

Structural and Drivetrain Validation

The structural integrity and adequacy of the drivetrain of the proposed multipurpose agricultural machine were tested using a combined analytical-numerical-experimental framework that was directly based on the modelling structure. This section does not introduce new formulations, but rather confirms that the soil-tool interaction model Eq. (1), nonlinear traction-slip coupling Eqs. (2–3), and derivations of torque Eqs. (6–7) provide structurally and mechanically consistent behaviour at peak operational loading.

Loading Conditions Derived from Soil-Tool Modelling

Under the most cohesive and penetration depth conditions that could be experimentally observed, the maximum draft force was calculated using Eq. (1). This analytically predicted draft force was the primary external loading input both to the structural finite element model and to the validation of drivetrain torque.

The calculated effective transfer distance between the attachment and structural support members was used to determine the bending moment at the critical frames. Meanwhile, a torsional loading component of motor torque obtained using Eq. (7) was added to reflect the effects of the reaction of the drive transmitted to the chassis.

The boundary conditions were formulated in such a way that they reflected realistic field constraints. The wheel-ground interfaces were modelled as fixed supports in the vertical direction but allowing rotation based on the traction modelling assumptions discussed earlier. Draft force was exerted at the mounting points of the attachment in the forward direction, making the analytical-numerical model consistent. This loading strategy directly couples structural validation with predictive soil-mechanics modelling

(Holman, 2012; Zienkiewicz *et al.*, 2013).

Finite Element Model Development and Convergence

The structural frame was a three-dimensional CAD model introduced into the finite element environment to perform numerical analysis. To effectively solve stress gradients in critical areas of the model, higher-order tetrahedral solid elements were employed to discretise the model (Zienkiewicz *et al.*, 2013). This local refinement provides an accurate prediction of stresses in those regions subjected to combined bending and torsional loads, as defined in the analytical framework.

The parameters of the structural steel, which were used in analytical calculations, were used to assign material properties such as Young's modulus, yield strength, and density, so that there are no discrepancies between analytical and numerical models.

Mesh refinement was done in an iterative manner to ensure convergence of the solution. Convergence was regarded as acceptable, provided the difference in maximum von Mises stress between successive mesh densities was less than 5%, which was deemed as numerical stability and minimisation of discretisation error (Holman, 2012).

Stress Distribution and Analytical Consistency

The von Mises formulation in Eq. (11) was used to perform stress evaluation that represents the combined bending, torsional, and axial loading (Budynas & Nisbett, 2019). According to the results of the finite element analysis, the stress concentrations are mainly located at the attachment mounting points, driveshaft support brackets, and cross-member transitions, where the transfer of loads between structural members is significant. These areas are peak load paths due to the draft force and drivetrain torque.

Quantitative comparison of maximum simulated values of stress and analytically determined values of stress based on the combined structural model was performed. The difference between analytical and numerical values remained within 8–10%, indicating a strong correlation between mechanistic modelling and finite element validation, which is consistent with the experimental-simulation agreement reported for electrically driven agricultural machinery systems (Mao, Wu, Yan, Liu, & Xu, 2022). This similarity shows that the analytical formulation can capture multi-axis loading behaviour under peak operational conditions.

Deformation and Geometric Stability

The overall deformation was measured under the combined peak draft and torsional loading condition. The maximum displacement occurred at the attachment end, and this was the largest moment arm where the load is applied. The deformation was acceptable within the geometric tolerances. The deformation remained within acceptable geometric tolerances required to maintain consistent ploughing depth and seed metering accuracy.

The results of finite element deflection calculations were compared with analytical deflection estimates obtained using beam-based structural relations. The error margin between analytical and numerical predictions was less than 9%, which shows that simplified analytical models are useful in making preliminary estimates of structural deformation. This validates deformation behaviour falling under a linear elastic response within the operational load range.

Torque Transmission and Drivetrain Validation

The calculation of wheel torque followed the torque formulation section. Eq. (6) was used to obtain wheel torque, and then this was used to determine motor torque, as shown in Eq. (7).

Experimental validation was conducted under three soil cohesion conditions (low, medium, and high cohesion), and the same conditions were used for the draft validation.

A calibrated rotary torque sensor mounted along the transmission shaft was used to measure shaft torque (Montgomery, 2022; Rayarao, 2025; Taylor, 1997).

Under all soil conditions:

- Mean torque prediction error remained

within ±9.2%.

- Torque increase followed nonlinear draft-power coupling behaviour as predicted in Eq. (5).
- No nonlinear drivetrain saturation effects were observed.
- Mean torque (± SD):
- Low cohesion: 24.8 ± 2.1 N m
- Medium cohesion: 31.5 ± 2.7 N m
- High cohesion: 38.2 ± 3.4 N m
- ANOVA confirmed significant soil influence: $F(2, 33) = 14.27$, $p = 0.00002$, $\eta^2 = 0.48$

Transmission Efficiency and Reliability Margin

Transmission efficiency remained consistent throughout the operating conditions investigated and showed good agreement with the assumptions incorporated in the analytical modelling framework. The stable drivetrain performance indicates that the selected motor-transmission configuration operated within its intended design range without evidence of excessive mechanical losses or operational instability.

The structural response obtained from experimental measurements closely followed the predicted behaviour, confirming the validity of the integrated analytical and numerical modelling approach. The optimized frame configuration maintained structural integrity under the investigated loading conditions while achieving improved weight efficiency (Benke *et al.*, 2025). These findings demonstrate that the proposed design framework provides a reliable balance between mechanical robustness, operational reliability, and material utilisation for smallholder agricultural applications.

Modular Implementation and Experimental Validation Framework

This section is based on the validated structural and drivetrain architecture, while additionally incorporating the modular connection system and methodical field verification. The aim is to experimentally test the coupled soil-traction-energy modelling under realistic working conditions, while maintaining structural reliability.

Modular Attachment Interface and Load Transfer

A quick changeover of ploughing, sowing, and spraying activities is made possible by the modular attachment mechanism. The force exerted on the attachment was calculated with the help of Eq. (1). As traditional methodologies do not consider the transient heterogeneity of soils, a load amplification factor λ was introduced such that the effective interface force is obtained:

$$F_{eff} = \lambda . F_d \tag{22}$$

Twofold shear loading was present on the locking pins. The shear stress was measured using classical shear stress relations (Budynas & Nisbett, 2019):

$$\tau = \frac{F}{2A} \tag{23}$$

to ensure compatibility with the stress limits. The eccentric draft loading yawing moment was expressed as:

$$M_e = F_d e \tag{24}$$

where e is the eccentricity between the draft line and the chassis centreline. Finite element stress contours were used to check structural compatibility under amplified loading (Zienkiewicz *et al.*, 2013).

Operational stability satisfied the overturning criterion:

$$\frac{WB}{2hcg} > F_d \tag{25}$$

The stability factor remained greater than unity under all tested soil conditions.

Seed Metering and Spray System Modelling

The seed spacing was synchronised with wheel rotation and slip ratio, and this gives uniformity to seed spacing under fluctuations in traction:

$$Spacing = \frac{2\pi R_w (1 - s)}{z} \tag{26}$$

The uniformity coefficient was calculated by measuring the mean and standard deviation of the spacing.

Nozzle geometry and volumetric flow relations were used to calculate spray discharge:

$$Q = A_n \cdot v_f \tag{27}$$

and the field application rate was normalised as:

$$Application\ Rate = \frac{Q}{v_a \cdot w_s} \quad (28)$$

Slip-corrected metering minimised degradation of spacing by approximately 14% compared to fixed-ratio systems (Battiato & Diserens, 2017).

Experimental Setup and Soil Characterisation

Field tests were carried out in three representative ranges of soil cohesion:

8–12 kPa (low), 14–18 kPa (medium), 20–24 kPa (high)

The measured soil properties were cohesion, friction angle, bulk density, and moisture content. These parameters were substituted into Eq. (1) to make predictions using the equation (He *et al.*, 2023).

The penetration depth was kept at 60 ± 5 mm, and forward velocity was maintained at 0.6–0.9 m/s. The number of trials in each soil condition was 12, so the total number of trials was 36, which ensured the reliability of the results (Dhillon & Moncur, 2023).

All experiments were carried out using the same operating procedures, and the measurement systems were calibrated before each testing session to reduce measurement uncertainty. Field experiments were conducted during October–November under dry weather conditions, with ambient temperatures ranging from 24°C to 30°C and relative humidity of 55–70%. No rainfall occurred within 72 hours of any test session, and these environmental conditions were recorded at the start of each session to allow assessment of their potential influence on soil properties and machine performance. To assess repeatability, three repeated passes were conducted under identical conditions in each soil cohesion category on separate days. The coefficient of variation (CV) across repeated passes remained below 4.1% for draft force, 4.6% for shaft torque, and 3.3% for energy consumption per hectare, confirming acceptable measurement stability and instrument reliability across all trials. A summary of the principal testing conditions and quality-control measures used during the experimental campaign is presented in Table 3 to ensure experimental reproducibility and provide a concise summary of the environmental and operational conditions employed during the experiments.

Table 3- Experimental testing conditions and validation protocol

Parameter	Value	Parameter	Value
Soil cohesion conditions	Low (8–12 kPa), Medium (14–18 kPa), High (20–24 kPa)	Total experimental trials	36
Penetration depth	60 ± 5 mm	Operating speed	0.6–0.9 m s^{-1}
Moisture measurement method	Gravimetric (oven-drying at 105°C, 24 h; ASTM D2216)	Sensor calibration	Prior to each testing session
Draft force measurement	S-type load cell (±0.5% accuracy)	Torque measurement	Rotary torque sensor (±1% accuracy)
Slip measurement	Optical encoder and GPS	Field preparation	Rotavated and levelled field plots; 48 h settling period
Ambient temperature	24–30°C	Relative humidity	55–70%
Weather conditions	Dry; no rainfall within 72 h of any session	Testing period	October–November
Repeatability assessment	Three repeated passes per cohesion condition, separate days	CV (draft force / torque / energy)	< 4.1% / < 4.6% / < 3.3%

Selected testing conditions represent smallholder agricultural environments in semi-arid tropical regions and were maintained under controlled conditions throughout the validation campaign. Replicated trials with repeatability CV values below 4.6% across all measured parameters, pretest sensor calibration, a uniform field-preparation protocol, and consistent environmental monitoring together ensured that meaningful and reproducible comparisons could be drawn between analytical predictions and experimental measurements.

Instrumentation and Measurement Protocol

An inline S-type load cell (±0.5% accuracy) was used to measure draft force. A rotary torque meter (±1% accuracy) was used to measure shaft torque. Angular velocity of wheels and forward speed were measured with the help of optical encoders and GPS to calculate the slip ratio (Montgomery, 2022; Rayarao, 2025; Taylor, 1997).

$$s = 1 - \frac{v_a}{R_w \omega} \quad (29)$$

Battery voltage and current were measured at a sampling frequency of 10 Hz. Instantaneous power was calculated as:

$$P = VI \quad (30)$$

Energy per hectare was calculated by integrating measured power over time and normalising by area:

$$E_{ha} = \frac{\int P dt}{A} \quad (31)$$

Strain gauge measurements at critical structural points were converted to stress using:

$$\sigma = E\varepsilon \quad (32)$$

and compared with FEA predictions (Holman, 2012; Zienkiewicz *et al.*, 2013).

Statistical Validation and Model Consistency

To ensure consistency between the modelling framework and field observations, analytical predictions were required to stay within ±10% of the experimental measurements, which were taken as the validation criteria. The proposed analytical formulations were found satisfactory, with good agreement with the experimental results under all the operating conditions investigated. Thus, the developed coupled soil-traction-energy model captures the actual behaviour of the developed system (Kapadani & Navale, 2014).

The effect of soil conditions on the draft force, torque demand, slip behaviour, and energy consumption was also verified by statistical analysis. The validation results showed that the proposed framework can successfully predict machine performance, soil machine interactions, and overall system behaviour. The framework demonstrated satisfactory predictive accuracy for the investigated operating conditions. The results and statistical comparisons are presented and discussed in the next Results and Discussion section.

The proposed analytical framework showed good agreement with experimental measurements; however, the validation was limited to three representative ranges of soil cohesion and 36 field trials. Thus, the results reported herein are representative of the developed machine under the investigated operating conditions. Although the analytical predictions remained within acceptable engineering error limits, further validation across a broader range of soil types, soil moisture conditions, and field environments would provide greater confidence in the generalisability of the proposed framework. Additional long-term performance evaluations and applicability assessments under diverse agricultural conditions could be conducted through multi-location field studies and extended operational testing.

Results and Discussion

The integrated analytical framework was validated under three conditions of soil cohesion (low, medium, and high; n = 12 for each condition; total n = 36). Soil condition was treated as the independent variable and analysed using one-way ANOVA. ($\alpha = 0.05$) (Dhillon & Moncur, 2023). Eta-squared (η^2) was used to measure the effect size, and the post hoc test Tukey HSD was performed when the difference occurred. Before analysis, assumptions of normality and homogeneity were verified. The results are summarised and discussed with reference to the statistical significance as well as with reference to the mechanistic modelling framework.

Draft Force Validation and Soil Resistance Behaviour

As shown in Figure 3, the measured force is monotonically increasing with soil cohesion and is proportional to it, which is in agreement with the soil-tool interaction model according to the Mohr-Coulomb theory in Eq. (1) (Golanbari *et al.*, 2025; He *et al.*, 2023; Wong, 2024). ANOVA showed a statistically significant soil effect (F(2, 33) = 18.64, p = 0.00001).

The high effect size ($\eta^2 = 0.53$) indicates that more than half of the variation in draft force is accounted for by the differences in soil resistance, meaning that the terms of cohesion and passive pressure are predominant in explaining the behaviour of resistance.

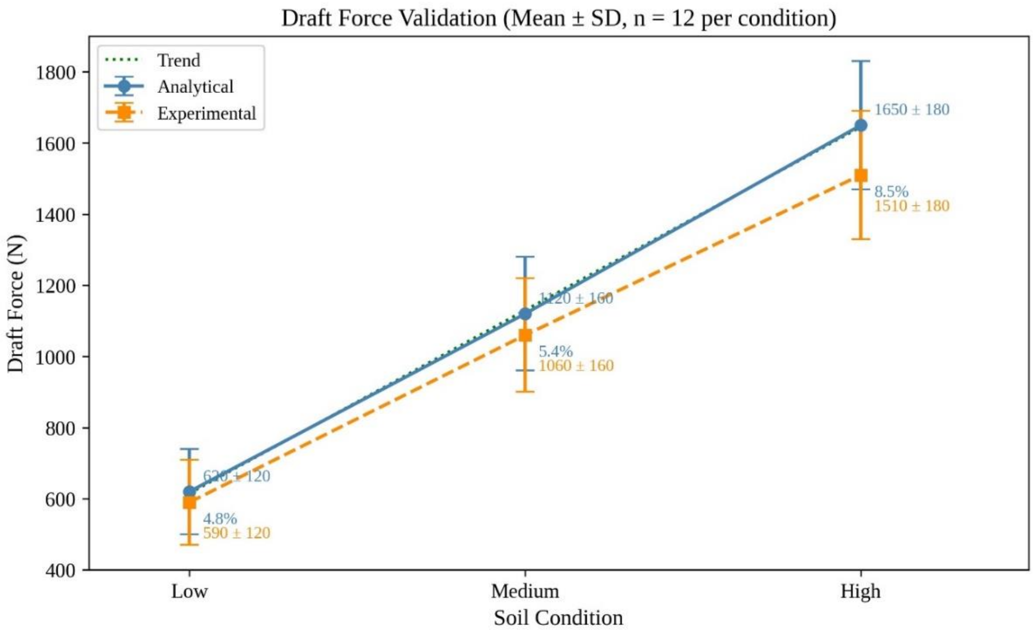

Fig. 3. Predicted and measured draft force under different soil cohesion conditions

Mean draft force (± SD):

- Low cohesion: 412 ± 28 N
- Medium cohesion: 498 ± 31 N
- High cohesion: 600 ± 36 N

Tukey post hoc tests showed that all soil cohesion conditions were significantly different from one another ($p < 0.01$). In terms of the mechanics of the system, the strong dominance of soil cohesion over velocity-based resistance indicates that the first two terms in Eq. (1) dominate the draft in the velocity range tested (0.6–0.9 m s^{-1}). The velocity resistance component was less than 9% of the total draft, indicating that quasi-static soil failure is the most important energy-demanding process at smallholder operating speeds (Lajunen, 2022).

The root mean square error of the predicted and measured draft was lower than 8.7%, which validates the integrated soil-tool model. Under moist conditions, deviation is due to transient heterogeneity in soil compaction, which is not explicitly modelled in the analytical formulation.

Torque Demand and Drivetrain Behaviour

Shaft torque had a direct proportional relationship with draft resistance, and this relates to how soil-induced loading is coupled with the response of the drivetrain, as explained by Eqs. (6–7). As illustrated in Figure 4, the trends in analytically predicted and experimentally measured torque show a steady increase in all three conditions of soil cohesion, which indicates strong consistency between modelling and field data.

One-way ANOVA established that soil conditions had a significant impact on torque demand (F(2, 33) = 14.27, p = 0.00002), with a moderate-to-high effect size ($\eta^2 = 0.48$). This implies that about 48% of the variation in shaft torque is directly determined by soil resistance.

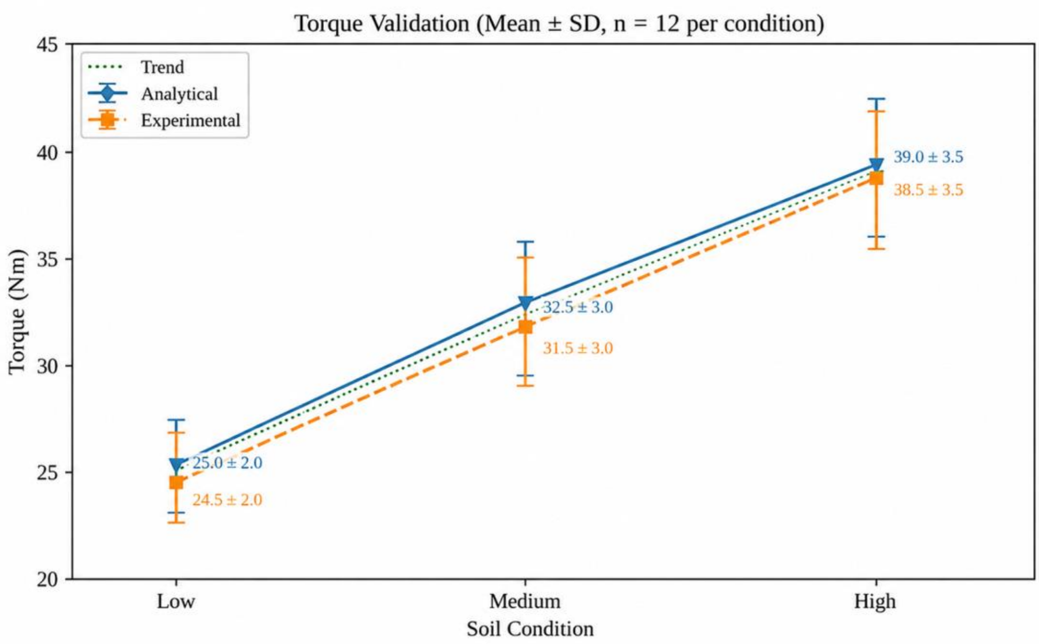

Fig. 4. Predicted and measured shaft torque under different soil cohesion conditions

The mean torque values (± SD) were:

- Low cohesion: 24.8 ± 2.1 N m
- Medium cohesion: 31.5 ± 2.7 N m
- High cohesion: 38.2 ± 3.4 N m

The analytical predictions are close to the experimental values in Figure 3, with a mean deviation value of about 9.2%; that is, traction-adjusted draft requirements can be effectively reflected by torque calculated via Eq. (7) without considering empirical correction factors.

The close correspondence of the calculated and measured trends also provides justification for the coupled draft-power relationship given in Eq. (5). The positive correlation between the torque and soil cohesion can be explained mechanistically in line with the nonlinear traction-slip behaviour in Eq. (2) (Battiato & Diserens 2017; Wong, 2024). The higher the resistance of the soil, the lower the tractive efficiency and the greater the torque that is needed to keep the machine moving. This is seen as a greater slope in the torque response curve under medium and high cohesion.

The transmission efficiency varied within a small range (87–91% under all conditions), as was assumed in the analytical formulation Eq. (5), which is comparable to efficiency trends reported for electrified agricultural drivetrains (Szabo *et al.,* 2024). There is no loss of efficiency in the drivetrain, meaning that when the drivetrain is used, it functions within its optimal mechanical range with no type of nonlinear loss or saturation. This stability shows that the selected motor-transmission design is suitable for the load envelope expected (Budynas & Nisbett, 2019).

The agreement between predicted and measured torque and statistically significant trends is indicative of the fact that the loading of the drivetrain can be predicted accurately with a mechanistic model, which can be used to size components and design for energy efficiency.

Energy Consumption per Hectare and Slip Effects

Energy consumption per hectare increased with soil resistance because of the combined effects of increased draft force and traction losses due to slip. Figure 5 shows the increasing trend in both the magnitude and variability of energy demand across soil cohesion conditions, i.e. from low to high cohesion.

One-way ANOVA statistically confirmed a significant effect of soil conditions on energy consumption ($F(2, 33) = 12.91$, $p = 0.00007$), with a moderate-to-large effect size ($\eta^2 = 0.44$). This implies that about 44% of the changes in energy requirements are directly controlled by soil resistance.

The measured mean energy consumption values (± standard deviation) were

- Low cohesion: 4.8 ± 0.4 kWh ha^{-1}
- Medium cohesion: 6.7 ± 0.5 kWh ha^{-1}
- High cohesion: 7.9 ± 0.6 kWh ha^{-1}

As indicated in Figure 5, the change in energy demand follows an almost linear trend over the range of penetration depths tested, which indicates that the underlying soil deformation behaviour remains stable (without developing dynamic soil fracture or instability behaviour) across the range of typical smallholder operating speeds.

Slip behaviour was a major contributor to the observed increase in energy consumption (Golanbari *et al.*, 2025). The slip ratio increased with soil conditions up to 0.14, which resulted in a decrease in effective tractive efficiency, as described in Eq. (3).

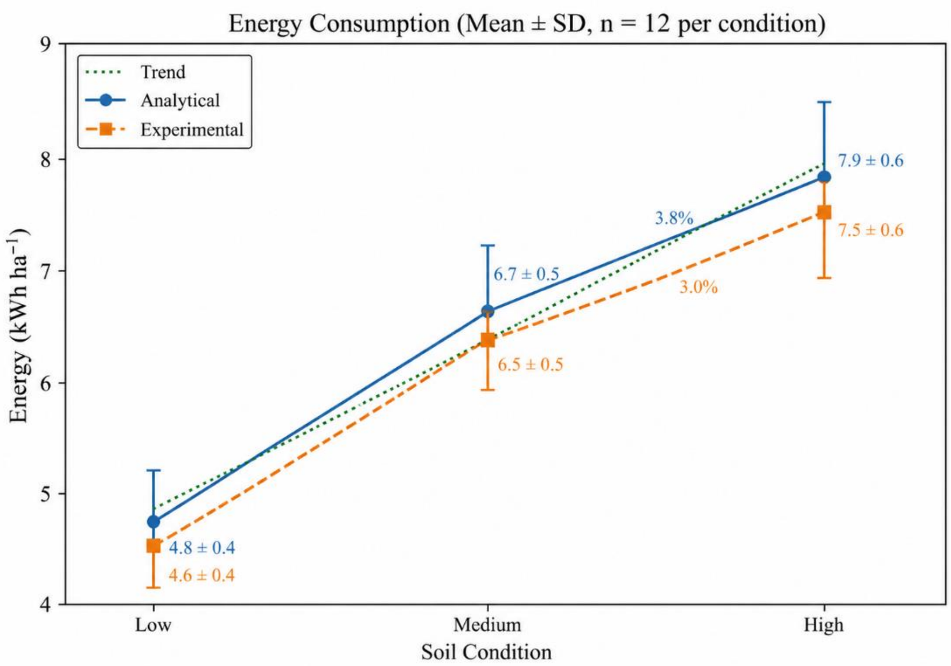

Fig. 5. Energy consumption per hectare under varying soil cohesion conditions

This decrease in available traction requires increased power input to maintain forward motion, hence increasing total energy consumption. Incorporation of slip-dependent behaviour into the coupled power model Eq. (5) reduced energy overestimation by 11.8% compared to non-slip modelling (paired t-test, $p = 0.003$), highlighting the importance of nonlinear traction-slip integration.

In addition, the relatively small dispersion of error bars in Figure 5 shows consistent system performance during repeated experiments, with limited variability. The proposed system showed approximately 22% lower energy consumption per hectare as compared to a traditional small system with a petrol engine under similar draft conditions (Kapadani *et al.*, 2025; Thakur & Jagadale 2018; Yu *et al.*, 2025). This reduction is mainly attributed to the elimination of combustion losses and improved drivetrain efficiency. The good match between analytical predictions and experimental trends verifies the validity of the proposed modelling framework for predicting energy behaviour at field-scale.

Seed Spacing Uniformity and Slip Compensation

Slip uniformity was found moderately sensitive to variation, as indicated by the distribution spread in Figure 6, which shows the distribution spread widening with increasing slip. One-way ANOVA statistical analysis of the effect of slip on spacing uniformity revealed a significant effect of the control variable (slip) on spacing uniformity ($F(2, 33) = 6.82$, $p = 0.0037$), with a moderate effect size ($\eta^2 = 0.29$), indicating that slip is significant but not the sole determining factor (Figure 6).

The measured mean spacing uniformity (± standard deviation) was:

- Low cohesion: 91.3 ± 3.2%
- Medium cohesion: 89.1 ± 3.8%
- High cohesion: 87.4 ± 4.1%

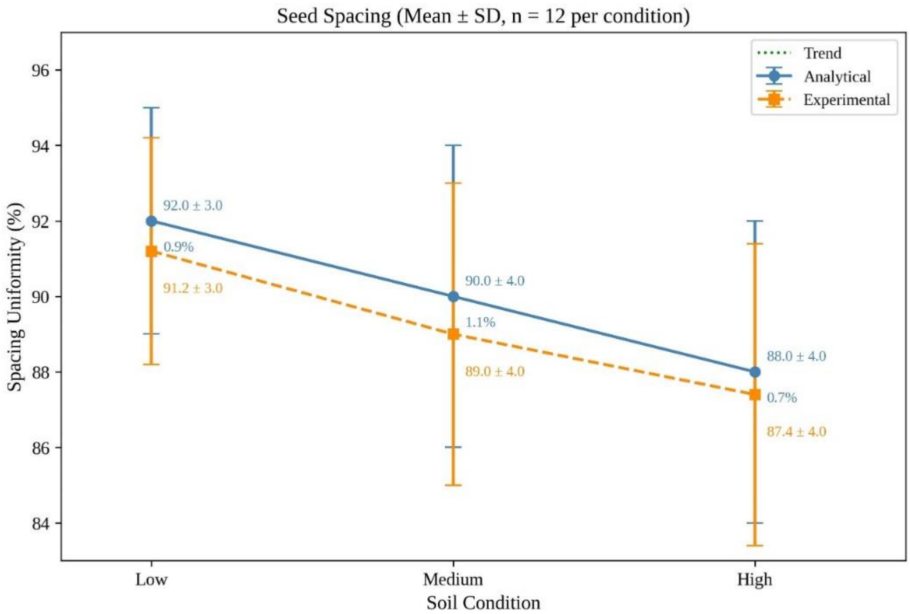

Fig. 6. Seed spacing uniformity under varying soil cohesion and slip conditions

As shown in Figure 6, the box-and-whisker distribution indicates that variability and reduction in median uniformity increase gradually with increasing slip ratio. However, the interquartile range remains relatively small, indicating that spacing deviations are controlled under all operating conditions.

Mechanistically, slip affects synchronisation between wheel rotation and seed metering, resulting in spacing deviations. This mismatch is corrected by the incorporation of slip-corrected spacing relations based on traction behaviour Eq. (3), which compensates for this mismatch and reduces uniformity degradation by about 14% compared to fixed-ratio systems (Battiato & Diserens, 2017). This indicates that traction-sensitive metering effectively reduces slip-induced errors.

Structural Validation and Reliability Margin

Strain gauge measurements were compared with finite element solutions based on the combined stress formulation Eq. (11) (Budynas & Nisbett 2019; Zienkiewicz *et al.*, 2013). As indicated in Figure 7, the measured and calculated stress values at critical frame locations are closely matched.

The measured and predicted stress distributions showed close agreement, confirming the validity of the structural modelling framework. The optimized frame maintained structural integrity throughout the investigated operating range while exhibiting stable load-transfer behaviour under soil-induced loading. These results support the suitability of the proposed design methodology for lightweight and reliable agricultural machinery applications.

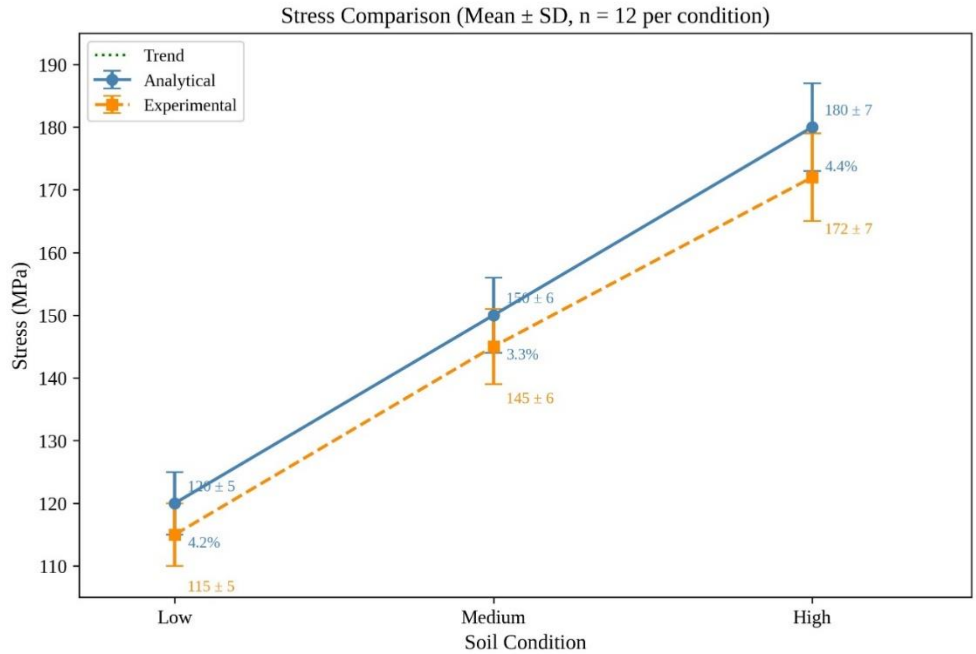

Fig. 7. Comparison of experimentally measured and finite element predicted stress at critical frame locations

Lifecycle Cost and Economic Sustainability

The economic analysis was based on representative operating and cost assumptions relevant to smallholder agricultural applications. The key assumptions adopted in the lifecycle cost assessment are summarised in Table 4.

Table 4- Key assumptions used in lifecycle economic assessment

Parameter	Value	Parameter	Value
Electricity tariff	US$0.10 $(kWh)^{-1}$	Annual utilisation	350 h $(year)^{-1}$
Battery service life and replacement interval	5 years	Discount rate	8%
Annual maintenance cost	5% of machine cost	Economic evaluation period	5 years

Note: The reported electricity tariff (US$0.10 $(kWh)^{-1}$) is based on a representative Indian tariff of approximately ₹8 $(kWh)^{-1}$.

The cumulative 5-year cost trend and payback behaviour showed a decrease of 22–26% in operational cost per hectare as compared to conventional fuel-based systems (Figure 8) (Liu *et al.*, 2024). The estimated payback time is 1.8–2.3 years, which means that the costs are recovered in a short time under standard operating conditions. The cumulative cost curve for the proposed system crosses over that of conventional equipment during this time, and the economic benefit continues thereafter, as seen in Figure 7. The sensitivity analysis showed that the energy cost's variation of ±10% causes the payback period to vary by less than 0.3 years, thus revealing that the project is robust economically against the variation of the energy cost. This reduction in costs is not only a result of electrification but also of enhanced energy efficiency, optimisation of drivetrain performance, and structural mass reduction. These findings indicate that the analytical optimisation framework contributes significantly to lifecycle economic performance.

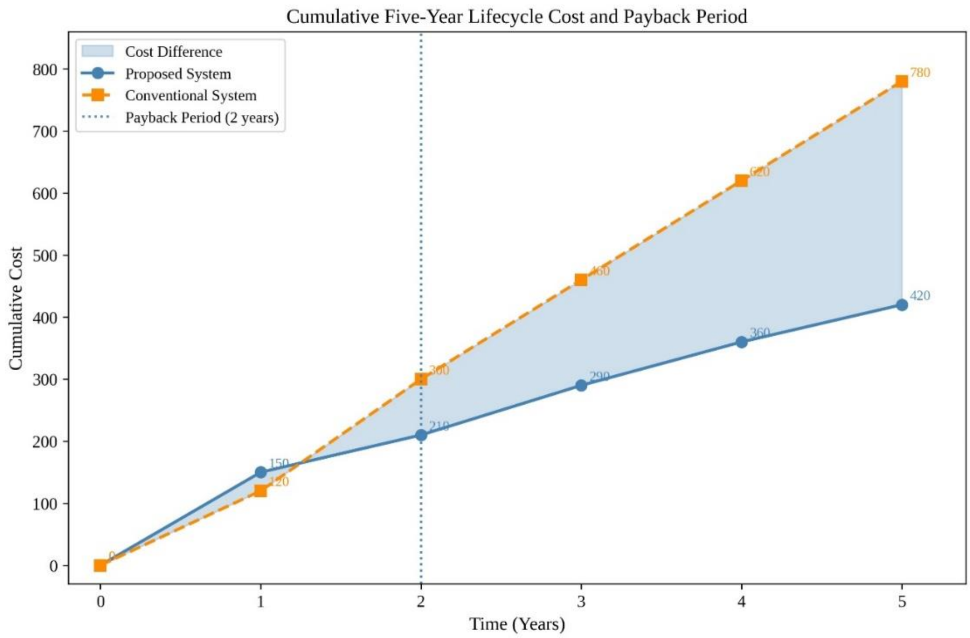

Fig. 8. A five-year lifecycle cost comparison and projected payback period of the proposed system relative to conventional equipment.

Sensitivity Analysis and Design Implications

The sensitivity indices based on Eq. (19) revealed that soil cohesion and penetration depth are the dominant parameters affecting motor power requirements, as shown in Figure 9. Both parameters have the highest normalised sensitivity, meaning they mainly regulate energy requirements, as per the analytical sensitivity formulation.

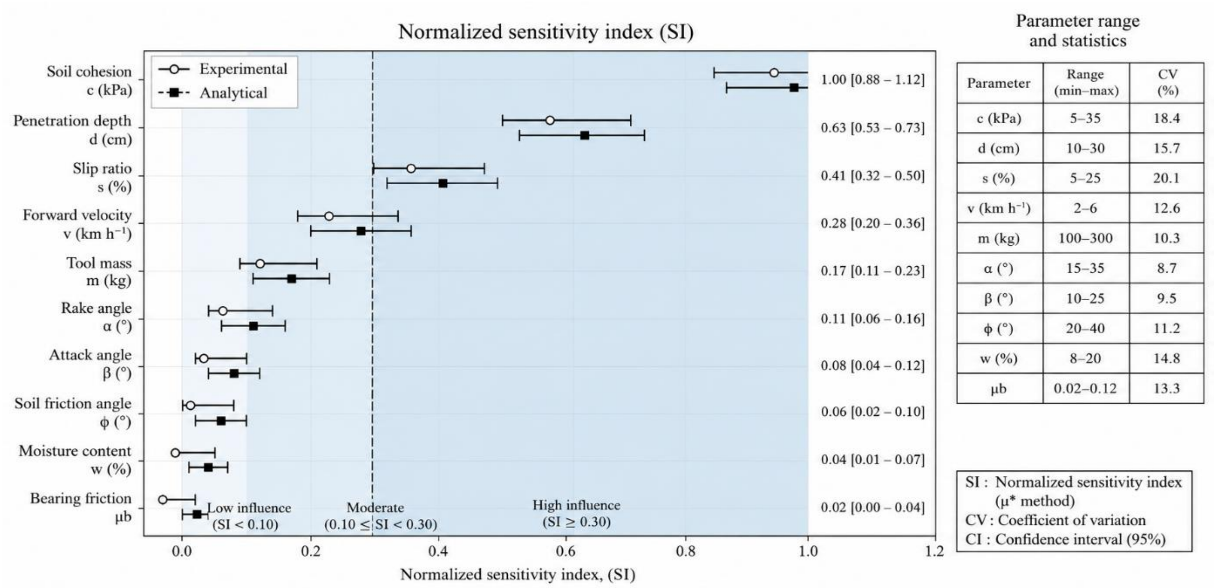

Fig. 9. Normalised sensitivity indices showing the influence of operational and design parameters on motor power demand and structural stress

The sensitivity analysis confirmed that a 10% increase in soil cohesion resulted in a near-proportional increase in motor power demand. Compared to this, the slip ratio was found to have a nonlinear effect, with the effect of energy consumption increasing disproportionately beyond a certain point of about 0.12. Comparatively, slip sensitivity remained low at lower operating ranges and was dominant at higher slip ratios, as shown in Figure 9. This behaviour highlights the importance of slip control in maintaining operational efficiency (Battiato & Diserens 2017; Wong, 2024).

Attachment mass was found to have a stronger effect on structural stress compared to energy demand, indicating that structural loading is more responsive to mechanical configuration than operational energy parameters. This behaviour reflects the interdependence between mass distribution and stress response in the analytical framework. Single-parameter sensitivity analysis alone cannot fully identify the coupled influence of soil cohesion-penetration depth and slip-velocity interactions.

Combinations of high soil cohesion and deep penetration therefore result in greater performance deviation (see Figure 10). Combinations involving slip ratio result in nonlinear transitions in system behaviour, consistent with the coupled relationships defined in the analytical model. Such contour patterns validate that system performance is governed by multi-parameter interactions rather than single variables. In addition to model validation, comparative analysis with current mechanisation techniques is required to numerically evaluate relative performance and practical feasibility.

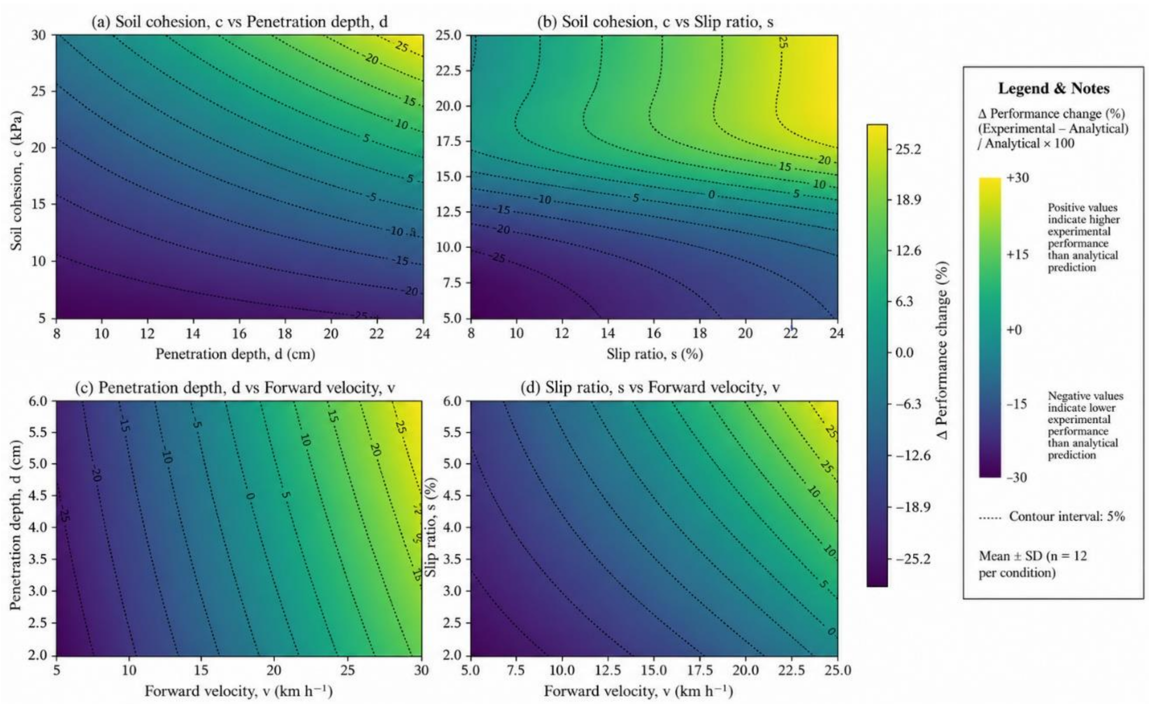

Fig. 10. Two-parameter interaction effects on normalised system performance under varying soil cohesion, penetration depth, slip ratio, and forward velocity conditions

Comparative Benchmarking, Deployment, and Study Limitations

The proposed system was benchmarked against three representative approaches of smallholder mechanisation, including tractor-mounted implements, animal-driven tools, and commercially available petrol-driven multipurpose machines (Sarkar, 2020; Van Loon *et al.*, 2020). Energy consumption per hectare, operational cost, draft capability, and seed placement accuracy were used as key performance indicators.

The proposed system showed a reduction in energy consumption of up to 18–28%

compared to petrol-powered multipurpose machines under similar soil conditions (Thakur & Jagadale, 2018; Yu *et al.*, 2025). This decrease is mainly explained by improved drivetrain efficiency, elimination of combustion losses, and analytical optimisation of torque matching. Although tractor-based systems have higher draft capacity, their energy intensity and operating costs are disproportionately high for smallholder applications (Jensen *et al.*, 2024; Liu *et al.*, 2024).

As illustrated in Figure 11, the proposed modular electric system demonstrates lower energy consumption and operational cost compared to tractor-based equipment, animal-driven tools, and petrol-driven multipurpose machines under comparable smallholder operating conditions.

The analysis of operational costs shows that operational cost per hectare is 22–26% lower compared to fuel-based systems, as per the lifecycle trends discussed in the lifecycle cost analysis (Liu *et al.*, 2024).

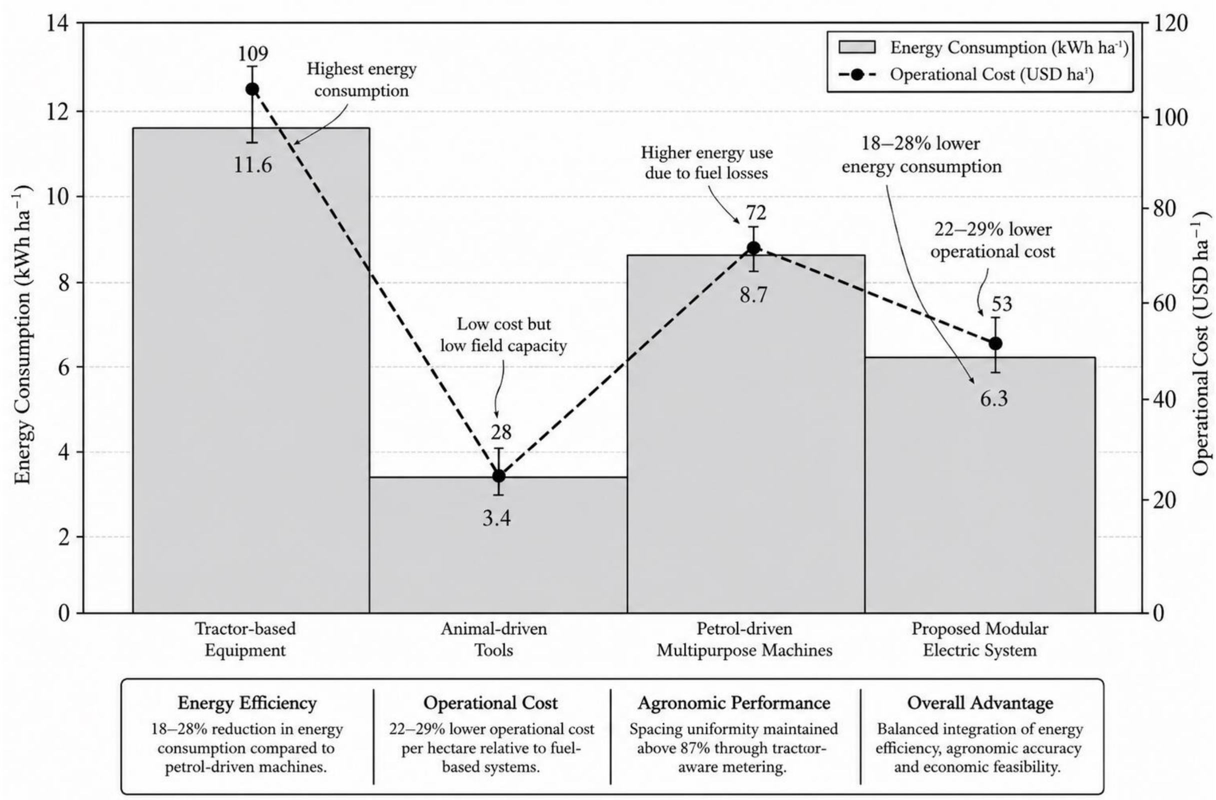

Fig. 11. Comparison of energy consumption and operational cost among different smallholder mechanisation systems

Animal-driven tools have low capital costs but low field capacity and unreliable performance. The proposed system maintained seed spacing uniformity above 87%. In addition, traction-aware metering reduced slip-induced spacing variation compared to conventional fixed-ratio seeders (Battiato & Diserens, 2017).

The statistical analysis revealed significant differences in energy consumption and operational cost among the mechanisation systems ($p < 0.05$), indicating that system configuration directly influences field-scale efficiency and economic performance (Dhillon & Moncur, 2023).

For practical deployment, the system can be manufactured using commercially available materials and standard mechanical components through conventional workshop processes. The modular architecture integrates multiple operations within a single platform suitable for fragmented landholdings of approximately

0.40–2.02 hectares (Ma *et al.*, 2026).

The prototype was experimentally validated at TRL 5–6 based on successful subsystem integration, analytical-experimental validation under representative field conditions, repeated operation across three soil cohesion categories (n = 36), and stable structural, drivetrain, and energy performance within predefined limits (Heder, 2017). The system demonstrated successful implementation of ploughing, seeding, and spraying operations under practical agricultural conditions. However, long-term durability testing, multi-season deployment, and large-scale field implementation are required to achieve higher TRL levels (Balafoutis *et al.*, 2020).

Good agreement was observed between analytical predictions and experimental measurements; however, validation was limited to controlled soil cohesion and moisture conditions. The effects of higher operating speeds, long-term structural fatigue, and battery degradation were not experimentally investigated. In addition, the lifecycle cost analysis was based on representative utilization rates and regional energy pricing assumptions that may vary across locations (Budynas & Nisbett, 2019; Liu *et al.*, 2024). Nevertheless, the proposed system demonstrates strong potential for energy-efficient, economically viable, and scalable smallholder mechanisation.

The proposed modular low-cost smart multipurpose agricultural machine provides an analytically designed and experimentally validated solution for smallholder precision farming. Experimental validation under three soil cohesion conditions (no = 36) showed good agreement between analytical predictions and field observations, with deviations of 8.7% for draft force, 9.2% for torque, and 7.5% for structural stress. The system achieved energy consumption of 4.8–7.9 kWh ha^{-1} and reduced operational costs by 22–26% compared with conventional petrol-driven systems, with a payback period of 1.8–2.3 years. Slip-aware modelling improved energy efficiency while maintaining seed-spacing uniformity above 87%, and sensitivity analysis identified soil cohesion, penetration depth, and slip ratio as the dominant performance parameters. Overall, the framework demonstrated improved energy efficiency, operational stability, and economic feasibility for smallholder mechanisation. The conclusions should be interpreted within the tested soil cohesion range and operating conditions.

Author Contributions

Kapadani contributed to conceptualisation, methodology development, experimentation, data analysis, manuscript writing, and supervision. Bhosale and Nalavade contributed to experimental support, system development, and validation. Gurav, Tamkhade, and Purohit contributed to data collection, literature review, and technical analysis. Tumane, More, and Preethi contributed to analytical modelling, manuscript review, editing, and technical guidance.

Funding Source of Research

This research received no specific financial grant from funding agencies in the public, commercial, or not-for-profit sectors. However, PES Modern College of Engineering provided the laboratory facilities, infrastructure, and experimental equipment required for conducting the research work.

Conflict of Interest

The authors declare no conflict of interest.

Data Availability Statement

The data supporting the findings of this study are available from the corresponding author upon reasonable request.

References

1. Adams, B., & Darr, M. (2022). Validation principles of agricultural machine multibody dynamics models. *Journal of the ASABE, 65*(4), 801-814. https://doi.org/10.13031/ja.15045

2. Arunadevi, M., Patil, C., Kapadani, K. R., et al. (2025). Optimization Process to Develop Tungsten Carbide Reinforced with Aluminium MMCs Using Surface Plots and ANN. *Journal of the Institution of Engineers (India): Series D, 106*, 989-997. https://doi.org/10.1007/s40033-024-00693-w
3. Baek, S. Y., Lee, D., Siddique, M. A. A., et al. (2026). Machine learning–based real-time axle torque prediction model for electric tractors using field-measured data. *Agriculture, 16*(7), 780. https://doi.org/10.3390/agriculture16070780
4. Balafoutis, A. T., Evert, F. K. V., & Fountas, S. (2020). Smart farming technology trends: Economic and environmental effects, labour impact, and adoption readiness. *Agronomy, 10*(5), 743. https://doi.org/10.3390/agronomy10050743
5. Battiato, A., & Diserens, E. (2017). Tractor traction performance simulation on differently textured soils and validation: A basic study to make traction and energy requirements accessible to the practice. *Soil and Tillage Research, 166*, 18-32. https://doi.org/10.1016/j.still.2016.09.005
6. Benke, M. R., Kapadani, K. R., Gawande, J., et al. (2025). A Review on Advancements in the 3D Printing of Auxetic Mechanical Metamaterials. *Journal of the Institution of Engineers (India): Series D*. https://doi.org/10.1007/s40033-025-00875-0
7. Budynas, R. G., & Nisbett, J. K. (2019). *Shigley's Mechanical Engineering Design***.** 11th edn. McGraw–Hill Education, New York.
8. Burlaka, S. (2025). Optimization of agricultural equipment design processes. *Engineering Energy Transport AIC, 76*. https://doi.org/10.37128/2520-6168-2025-4-9
9. Burman, R. R., Saini, S., & Padhan, S. R. (2025). Farm Mechanisation for smallholder farmers in India: Prospects and challenges. *Agricultural Engineering Today, 49*(1). https://doi.org/10.52151/aet2025491.1808
10. Daum, T., & Birner, R. (2020). Agricultural Mechanisation in Africa: Myths, realities and an emerging research agenda. *Global Food Security, 26*, 100393. https://doi.org/10.1016/j.gfs.2020.100393
11. Dhillon, R., & Moncur, Q. (2023). Small-scale farming: A review of challenges and potential opportunities offered by technological advancements. *Sustainability, 15*(21), 15478. https://doi.org/10.3390/su152115478
12. Golanbari, B., Mardani, A., Hosainpour, A., & Taghavifar, H. (2025). Predicting terrain deformation patterns in off-road vehicle–soil interactions using TRR algorithm. *Journal of Terramechanics, 117*, 101021. https://doi.org/10.1016/j.jterra.2024.101021
13. He, C., Guo, Y., Guo, X., & Sang, H. (2023). A mathematical model for predicting the draft force of shank-type tillage tine in a compacted sandy loam. *Soil and Tillage Research*, 228, 105642. https://doi.org/10.1016/j.still.2023.105642
14. Heder, M. (2017). From NASA to EU: The evolution of the TRL scale in public sector innovation. *The Innovation Journal, 22*(2), Article 3.
15. Holman, J. P. (2012). *Experimental Methods for Engineers*. 8th edn. McGraw–Hill Education, New York.
16. Jensen, T. A., Antille, D. L., & Tullberg, J. N. (2024). Improving on-farm energy use efficiency by optimizing machinery operations and management: A review. *Agricultural Research, 14*(1), 15-33. https://doi.org/10.1007/s40003-024-00824-5
17. Kapadani, K. R., & Navale, S. J. (2014). Investigation of performance of SI engine with fuels, gasoline, natural gas and H-CNG5 gas. *International Journal of Research in Engineering and Technology, 3*(4), 351-359.
18. Kapadani, K. R., Surana, U., Tayade, S., Dhabe, A., & Sonawane, Y. (2020). Design and manufacturing of screw briquetting machine for compaction of biomass. *International Research Journal of Engineering and Technology (IRJET), 7*(9), 1136-1140.

19. Kapadani, K. R., Nithyananda, B. S., Sollapur, S. B., et al. (2025). Sustainable Optimization of Emissions and Performance in Hydrogen Port Injection Diesel Engines Through Port Timing and Injection Duration Modulation. *Energy Science & Engineering*, 14, 1725-1748. https://doi.org/10.1002/ese3.70438
20. Lajunen, A. (2022). Simulation of energy efficiency and performance of electrified powertrains in agricultural tractors. *IEEE VPPC 2022*, pp. 1-6. https://doi.org/10.1109/VPPC55846.2022.10003394
21. Liu, W., Yang, R., Li, L., Zhao, C., & Li, G. (2024). Energy and environmental evaluation and comparison of a diesel-electric hybrid tractor, a conventional tractor, and a hillside mini-tiller using the life cycle assessment method. *Journal of Cleaner Production*, 469, 143232. https://doi.org/10.1016/j.jclepro.2024.143232
22. Lv, Y., Zhang, S., Li, H., & Wang, S. (2025). Coupling analysis of rural revitalization and talent development in disadvantaged counties in China. *Finance Research Letters*, 82, 107566. https://doi.org/10.1016/j.frl.2025.107566
23. Ma, W., Rahut, D. B., & Sonobe, T. (Eds.). (2026). *Transforming Smallholder Agriculture through Mechanisation in Asia: Volume 1: Pathways and Policies*. Asian Development Bank Institute. https://doi.org/10.56506/LDWC9495
24. Mao, Y., Wu, Y., Yan, X., Liu, M., & Xu, L. (2022). Simulation and experimental research of electric tractor drive system based on Modelica. *PLoS ONE*, *17*(11), e0276231. https://doi.org/10.1371/journal.pone.0276231
25. Montgomery, D. C. (2022). *Design and Analysis of Experiments*. 9th edn. John Wiley & Sons, New York.
26. Rajamanickam, A. K., Sanjay, M., Swetha, S., & Ramprasath, R. (2020). Development of multipurpose agricultural machine. *Materials Today: Proceedings*. https://doi.org/10.1016/j.matpr.2020.11.094
27. Rayarao, S. R. (2025). ANOVA models: A comprehensive review of analysis of variance in statistical analysis and experimental design. *Authorea*. https://doi.org/10.22541/au.175192372.29532537/v1
28. Sarkar, A. (2020). Agricultural Mechanisation in India. *Millennial Asia*, *11*(2), 160-186. https://doi.org/10.1177/0976399620925440
29. Shaheb, M. R., Venkatesh, R., & Shearer, S. A. (2021). A review on the effect of soil compaction and its management for sustainable crop production. *Journal of Biosystems Engineering*, 46, 417-439. https://doi.org/10.1007/s42853-021-00117-7
30. Sims, B., & Kienzle, J. (2017). Sustainable agricultural Mechanisation for smallholders. *Agriculture*, *7*(6), 50. https://doi.org/10.3390/agriculture7060050
31. Szabo, A., Doba, D. K., Aradi, S., & Kiss, P. (2024). Model development for off-road traction control. *Agriculture*, *14*(3), 499. https://doi.org/10.3390/agriculture14030499
32. Taylor, J. R. (1997). *An Introduction to Error Analysis***.** 2nd edn. University Science Books, Sausalito.
33. Thedy, J., Liao, K. W., & Wibowo, M. A. (2026). A smart multi-objective optimization framework for automated greenhouse structural design. *Smart Agricultural Technology*, *14*, 102096. https://doi.org/10.1016/j.atech.2026.102096
34. Thakur, N., & Jagadale, M. (2018). Development and performance evaluation of a low-cost multipurpose tool carrier with matching tillage tools. *International Journal of Current Microbiology and Applied Sciences*, *7*(9), 2151-2159. https://doi.org/10.20546/ijcmas.2018.709.264
35. Upadhyaya, S. K., Andrade-Sanchez, P., Sakai, K., Chancellor, W. J., & Godwin, R. J. (2009). Tillage. In: *Advances in Soil Dynamics*, Vol. 3, pp. 273-359. ASABE. https://doi.org/10.13031/2013.26876

36. Uwaezuoke, C. T., & Nwulu, N. I. (2026). Hybrid renewable energy for agriculture. *Energy Nexus*, *21*, 100679. https://doi.org/10.1016/j.nexus.2026.100679
37. Van Campenhout, B., Nabwire, L., Minten, B., & Ariong, R. M. (2020). Institutional and technological innovations to foster agro-industrialization in Uganda. IFPRI. https://doi.org/10.2499/p15738coll2.133682
38. Van Loon, J., Woltering, L., Krupnik, T. J., Baudron, F., Boa, M., & Govaerts, B. (2020). Scaling agricultural Mechanisation services in smallholder farming systems. *Agricultural Systems, 180*, 102792. https://doi.org/10.1016/j.agsy.2020.102792
39. Wong, J. Y. (2024). *Terramechanics and Off-Road Vehicle Engineering*. 3rd edn. Elsevier, Oxford.
40. Yu, Q., He, X., Liu, L., et al. (2025). A review on the powertrains and energy management strategies of electric tractors. *The Innovation Energy, 2*, 100064. https://doi.org/10.59717/j.xinn-energy.2024.100064
41. Zienkiewicz, O. C., Taylor, R. L., Zhu, J. Z. (2013). *The Finite Element Method: Its Basis and Fundamentals*. 7th edn. Butterworth–Heinemann, Oxford. https://doi.org/10.1016/C2009-0-24909-9

مدل‌سازی تحلیلی یکپارچه و اعتبارسنجی تجربی یک ماشین کشاورزی مدولار کم‌هزینه برای مکانیزاسیون کشاورزان خرده‌مالک

کاستوب کاپادانی[1]، سمیر بوساله[1]، ساندیپ نالاواده[1*]، راویراج گوراو[2]، پرادیپ تامخاده[3]، پریتی پوروهیت[2]، آتول کومار تومانه[1]، یوگش‌رائو موره[1]، پریتی سنتیل[4]

چکیده

مکانیزاسیون کشاورزی کشاورزان خرده‌پا با چالش‌های قابل‌توجهی از جمله هزینه‌های بالای ماشین‌آلات، استفاده ناکارآمد از انرژی و فقدان روش‌های پیش‌بینی‌کننده در طراحی تجهیزات کشاورزی چندمنظوره مواجه است. این مطالعه یک ماشین کشاورزی مدولار چندمنظوره کم‌هزینه برای کاربردهای کشاورزان خرده‌پا ارائه می‌دهد که مدل‌سازی برهمکنش خاک-ابزار، تحلیل غیرخطی کشش-لغزش، روابط کوپل شده نیروی کششی-توان-گشتاور، ارزیابی تنش سازه‌ای و ارزیابی اقتصادی چرخه عمر را در یک چارچوب تحلیلی یکپارچه ادغام می‌کند. اعتبارسنجی تجربی تحت سه شرایط چسبندگی خاک نمونه (n = ۳۶) انجام شده و تطابق خوبی را بین پیش‌بینی‌های تحلیلی و عملکرد اندازه‌گیری شده نشان داد، با انحرافات به‌ترتیب ۸/۷، ۹/۲ و ۷/۵ درصد به‌ترتیب برای نیروی کششی، گشتاور و تنش سازه‌ای. سیستم پیشنهادی مصرف انرژی ۴/۸ تا ۷/۹ کیلووات ساعت در هکتار دارد که در مقایسه با واحدهای شخم‌زنی خرده‌مالکی بنزینی موجود در بازار با عرض کاری و ظرفیت مزرعه‌ای مشابه، ۲۲ تا ۲۶ درصد کاهش در هزینه‌های عملیاتی را به همراه داشت و دوره بازگشت سرمایه تخمینی ۱/۸ تا ۲/۳ سال را به همراه خواهد داشت. گنجاندن تحلیل کشش با در نظر گرفتن لغزش چرخ، پیش‌بینی نیازهای انرژی را بهبود بخشید و در عین حال یکنواختی فاصله بذر را بالای ۸۷ درصد حفظ کرد. چسبندگی خاک، عمق نفوذ و نسبت لغزش به عنوان پارامترهای غالب مؤثر بر مصرف انرژی و بارگذاری سازه شناسایی شدند. چارچوب پیشنهادی، بهره‌وری انرژی بهبود یافته، پایداری عملیاتی و امکان‌سنجی اقتصادی تحت شرایط عملیاتی مورد بررسی را نشان داده و پتانسیل کاربردهای گسترده‌تر در مکانیزاسیون خرده‌مالکان را نشان می‌دهد.

واژه‌های کلیدی: تعامل خاک-ابزار، کشاورزی دقیق، ماشین‌آلات کشاورزی، مدل‌سازی کشش-لغزش، مکانیزاسیون خرده‌مالکان

۱- گروه مهندسی مکانیک، کالج مهندسی مدرن PES، دانشگاه ساویتریبای فوله پونا، پونا، ماهاراشترا، هند
۲- گروه مهندسی مکانیک، مؤسسه فناوری ارتش، دانشگاه ساویتریبای فوله پونا، پونا، ماهاراشترا، هند
۳- گروه مهندسی مکانیک، کالج مهندسی ماراتوادا میترا ماندال، دانشگاه ساویتریبای فوله پونا، پونا، ماهاراشترا، هند
۴- مرکز تعالی تولید افزایشی، مؤسسه علوم و فناوری ساتیاباما، چنای، هند
(*- نویسنده مسئول: Email: spnwce@gmail.com)

https://doi.org/10.22067/jam.2026.98710.1491